Journal of Sol-Gel Science and Technology (2020) 96:219–225
https://doi.org/10.1007/s10971-020-05379-9

ORIGINAL PAPER: SOL-GEL AND HYBRID MATERIALS FOR ENERGY, ENVIRONMENT AND BUILDING APPLICATIONS

Synthesis and electrocatalytic properties of $LaFe_{1-x}Zn_xO_3$ perovskites

Elies Omari[1] · **Mahmoud Omari**[1]

Received: 15 April 2020 / Accepted: 22 July 2020 / Published online: 30 July 2020

Abstract

In this work, perovskite-type oxides of general formula $LaFe_{1-x}Zn_xO_3$ ($0 \le x \le 0.3$) prepared by a sol–gel route were investigated as electrocatalysts for the oxygen evolution reaction (OER) in alkaline KOH solutions. X-ray diffraction analysis of samples indicates that the pure cubic structure was obtained for composition lower than $x = 0.2$. The OER studies indicate that substitution of iron by zinc increases the electrocatalytic activity of the resulting material significantly. The highest activity was achieved for $x = 0.1$, whereas the obtained current density was 9.02 mA cm^{-2} at 0.66 V, which is approximately three times higher than that of the base oxide. The Tafel slopes values for OER on each oxide in 1 M KOH are found to be ~89, 52, and 64 mV dec^{-1} for $LaFeO_3$, $LaFe_{0.9}Zn_{0.1}O_3$, and $LaFe_{0.8}Zn_{0.2}O_3$, respectively. The stability of $LaFe_{0.9}Zn_{0.1}O_3$ electrode is studied in the process of 1000 successive cycles at a current density of 10 mA.cm^{-2} of the OER. A small change in overpotential was found, ranged between 11 and 19 mV, indicating clearly its long electrochemical durability. These results suggest clearly that $LaFe_{0.9}Zn_{0.1}O_3$ electrode is a promising anode material for the OER in water electrolysis.

Graphical Abstract

Linear sweep voltammetry of $LaFe_{1-x}Zn_xO_3$ electrodes in 1 M KOH, at a scan rate of 50 mV/s; inset shows the OER current density at 0.66 V vs. Hg/HgO.

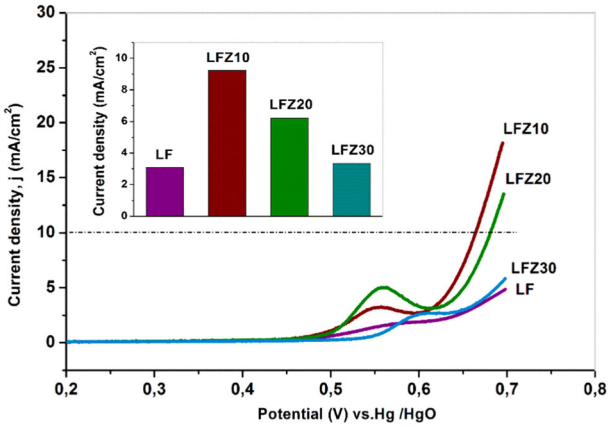

Keywords $LaFe_{1-x}Zn_xO_3$ perovskite oxides · Electrocatalytic activity · Oxygen evolution reaction · Electrode stability

✉ Mahmoud Omari
m2omari@yahoo.fr

[1] Laboratory of Molecular Chemistry and Environment, University of Biskra, B.P 145 07000 Biskra, Algeria

Highlights

- Perovskite-type oxides $LaFe_{1-x}$ Zn_xO_3 were used for oxygen evolution reaction.
- The highest elctrode activity performance is acheived with $LaFe_{0.9}Zn_{0.1}O_3$ at 0.66 V.
- The best performing electrode exhibits a relatively excellent stability after 1000 continuous cycles.

1 Introduction

Actually, global demand for energy is increasing rapidly because of population and economic growth particularly in emerging countries. The whole human population over the world depends generally on the energy produced from petroleum derivatives. However, the amount of carbon-based fuels diminishes and pollution of environment have drawn the attention of researchers toward sustainable and nonconventional sources and fuels [1, 2]. To resolve the energy crisis and reduce the emission of pollution, the utilization of hydrogen (H_2) is an essential renewable energy carrier. In the fuel cell, it is combined to oxygen for generating electricity and forms only water, which makes it environmental friendly [3]. Production of H_2 from steam reforming of methane is a dominant method and produces H_2 in large quantity altogether with gases such as carbon dioxide and carbon monoxide [4]. In the same context, water electrolysis is one of cleanest ways available capable of providing large amounts of the renewable hydrogen. In practice, the efficiency of water electrolysis is limited by kinetically slow oxygen evolution reaction (OER), since the anodic reaction is usually slower than cathodic reaction [5–7]. The large anodic overpotential during the electrolysis and high activation in aqueous solution are the main factors that affect the OER rate. Therefore, the main objective of the current research is to understand the OER kinetics and reduce the over potential in alkaline media. Many works have been made in the past to use electrocatalysts for enhancing the electrochemically active area. Traditionally, various mixed oxides such as IrO_2, RuO_2, and TiO_2 have been used frequently as catalysts for OER, which often showed the best catalytic activity and less stability under alkaline electrolyte as well as high cost [8]. During recent years, increasing attention has been directed now to search high active and stable OER catalysts based on cheaper metals such as oxides and hydroxides based of transition metals (Ni, Co, Fe, etc.) [9–11].

Perovskite-type oxides with the general formula ABO_3 are estimated as active electrocatalysts for OER reaction, owing to their high catalytic activity [12]. The partial replacement of A or/and B sites by suitable metal ions is responsible for the thermal resistance and catalytic activity, respectively [13]. Several studies have been carried out on the OER performance of pure and substituted of $LaFeO_3$ perovskites. Sankannavar et al. have reported that substitution of lanthanum by calcium increases the average oxidation state of iron from Fe^{3+} to Fe^{4+} and creates oxygen vacancies [1]. Another works have mentioned that Fe^{4+} ion is the OER active site on iron oxides [14–16]. Moreover, Suntivich et al. [17] have reported that the high OER activity of perovskite oxides is due to e_g occupancy close to unity of B site transition metal. Zinc was used as dopant in several works. This choice is justified by its abundance, ability to produce extrinsic defects [18] and its important role in enhancing electrocatalytic performances for OER [19].

Despite all these advantages, $LaFe_{1-x}Zn_xO_3$ oxides have been subject of few works. Huang et al. have studied the sensitivity of $LaFe_{1-x}Zn_xO_3$ to formaldehyde, shown that Zn-doping enhances the gas sensitivity of $LaFeO_3$ [20]. Two years later, Dong et al. have investigated the photocatalytic properties of these materials for the degradation of methylene blue. It has been found that the $LaFe_{0.7}Zn_{0.3}O_3$ sample exhibits the highest degradation rate of 75% under irradiation time of 150 min [21]. Thereafter, Bhat et al. have synthesized using sol–gel auto-combustion process, characterized magnetic and dielectric properties of $LaFe_{1-x}Zn_xO_3$ oxides [22]. To our best knowledge, there is no report in the literature on the electrocatalytic properties of $LaFe_{1-x}Zn_xO_3$ for the OER. In our present work, first row transition metal (Fe and Zn) based perovskite materials $LaFe_{1-x}Zn_xO_3$ ($0.0 \leq x \leq 0.3$) were synthesized by a typical sol–gel route. The electrocatalytic activity and the kinetics of the OER on the doped zinc lanthanum ferrites electrodes were investigated using linear sweep voltammetry (LSV), cyclic voltammetry (CV), Tafel slopes, and electrochemical impedance spectroscopy (EIS).The electrochemical stability analysis of $LaFe_{1-x}Zn_xO_3$ electrodes was also performed under OER conditions over 1000 cycles.

2 Materials and methods

2.1 Preparation of $LaFe_{1-x}Zn_xO_3$ catalysts

$LaFe_{1-x}Zn_xO_3$ powders, which can be named LF ($x = 0.0$), LFZ10 ($x = 0.1$), LFZ20 ($x = 0.2$), LFZ30 ($x = 0.3$), were prepared by citrate sol–gel method with employed lanthanum, zinc, iron nitrates as starting materials and citric acid as a complexant agent. Precursors $La(NO_3)_3{\cdot}6H_2O$, $Fe(NO_3)_3.9H_2O$, $Zn(NO_3)_2.6H_2O$ dissolved in ethanol were well-mixed under vigorous stirring, subsequently, citric acid was added into the above mixture. The resulting

homogeneous mixture was heated at 60–70 °C with continuous stirring until a violet red transparent solution was obtained, becomes gradually viscous, and later the amorphous gel was formed. To remove residual ethanol, the gel was dried in an oven at 100 °C for 24 h. Finally, the $LaFe_{1-x}Zn_xO_3$ powders were further calcined at 750 °C under air atmosphere for 6 h.

2.2 Catalysts characterization

The crystallographic information on the $LaFe_{1-x}Zn_xO_3$ ($0.0 \le x \le 0.3$) oxides were recorded by a powder X-ray diffractometer (D8 ADVANCED-BRUCKER) equipped with CuK_α as the radiation ($\lambda = 1.542$ Å) at a sweep rate of $2° \text{ min}^{-1}$ from 10 to 90°. X'pert High-Score plus software (version 2.1.0) was used for the phase identification of powders by comparing with the International Centre for Diffraction data. Moreover, morphological aspects of the powders were examined by scanning electron microscopy (SEM) (model VEGA 3 TESCAN).

2.3 Electrode preparation

The oxide electrocatalysts prepared in powder form were reproduced in the form of film on a pretreated nickel support by an oxide-slurry painting method. Prior to use, Ni plates (2 × 1 cm) were etched for 10 min in concentrated HCl, washed with double distilled water, degreased in acetone, and then dried in air. The powder was dispersed in ethanol by subsequent ultra-sonication of the mixture for 30 min and then stirred in an oven at 90 °C. A pure nickel plate was coated by a thin layer of oxide powder, then heating at 100 °C for 2 h in an electrical furnace to sinter the binder particles. The oxide load on the electrode was ~15 mg cm^{-2}.

2.4 Electrochemical measurements

A three-electrode single compartment pyrex glass cell was used to carry out electrochemical investigations with a potentiostat–galvanostat (model Parstat 4000). The reference and auxiliary electrodes are Hg/HgO and Pt, respectively. All potential values mentioned in the text have been referred to this reference electrode. Procedure followed in the study of LSV, CV, anodic Tafel polarization has already been described elsewhere [23, 24]. The EIS study of the oxide film electrodes in 1 M KOH has been carried out with an ac voltage amplitude of 5 mV over the frequency range of 0.01–10^4 Hz at varying potentials (0.60–0.68 V). The stability of LF and LFZ10 electrodes was studied after 1000 cycles of continuous CV scans with a scan rate of 20 mV/s.

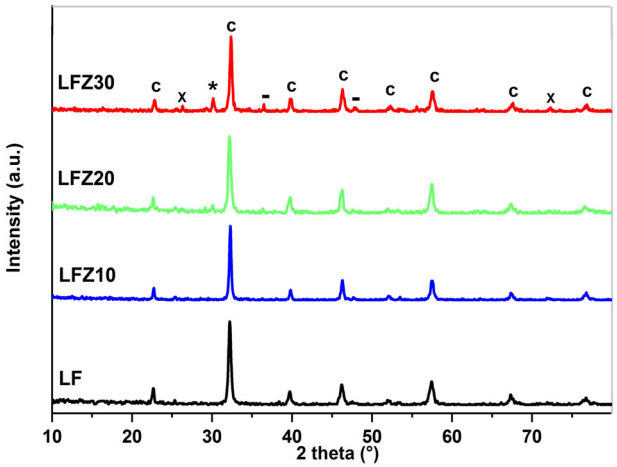

Fig. 1 X-ray diffraction patterns of synthesized $LaFe_{1-x}Zn_xO_3$ ($x =$ 0.0–0.3) after calcination at 750 °C, c: cubic phase; *: $ZnFe_2O_4$; −: ZnO; X: La_2O_3

3 Results and discussion

3.1 Structural characteristics of $LaFe_{1-x}Zn_xO_3$ catalysts

Figure 1 presents XRD patterns of the calcined samples $LaFe_{1-x}Zn_xO_3$ ($0 \le x \le 0.3$) at 750 °C for 6 h. The samples LF and LFZ10 exhibit a pure perovskite phase with a cubic structure (JCPDS:01-075-0541). At high zinc content ($x \ge$ 0.2), new peaks appear with weak intensity corresponding to $ZnFe_2O_4$ (JCPDS: 01-073-1963), ZnO (JCPDS: 01-075-1526), and La_2O_3 (JCPDS: 00-002-0688). This result is consistent with a previous report which indicates that $LaFe_{1-x}Zn_xO_3$ exhibit a pure cubic perovskite up $x = 0.1$ [21]. A slight shift of peaks can be observed with increasing the amount of zinc, which is probably due the difference between ions radius of Fe^{3+} (0.64 Å) and Zn^{2+} (0.74 Å).

3.2 Scanning electron microscopy

The morphologies of the pure and doped of $LaFeO_3$ powders studied by SEM are shown in Fig. 2. The micrographs images indicate that particles shapes are not well defined. It seems to consist of macro-agglomerations of numerous nano-crystallite particles with varying shape and grain sizes (particle–particle interactions). In this case, all the compounds show a non-uniform distribution with some clustered particles. The formation of agglomerates is likely due to the nature of the solvent used in the preparation of the gel. Moreover, the surface morphologies of these zinc-doped ceramics are dense, which is probably due to the particles that have a high tendency of agglomeration with interconnected structure.

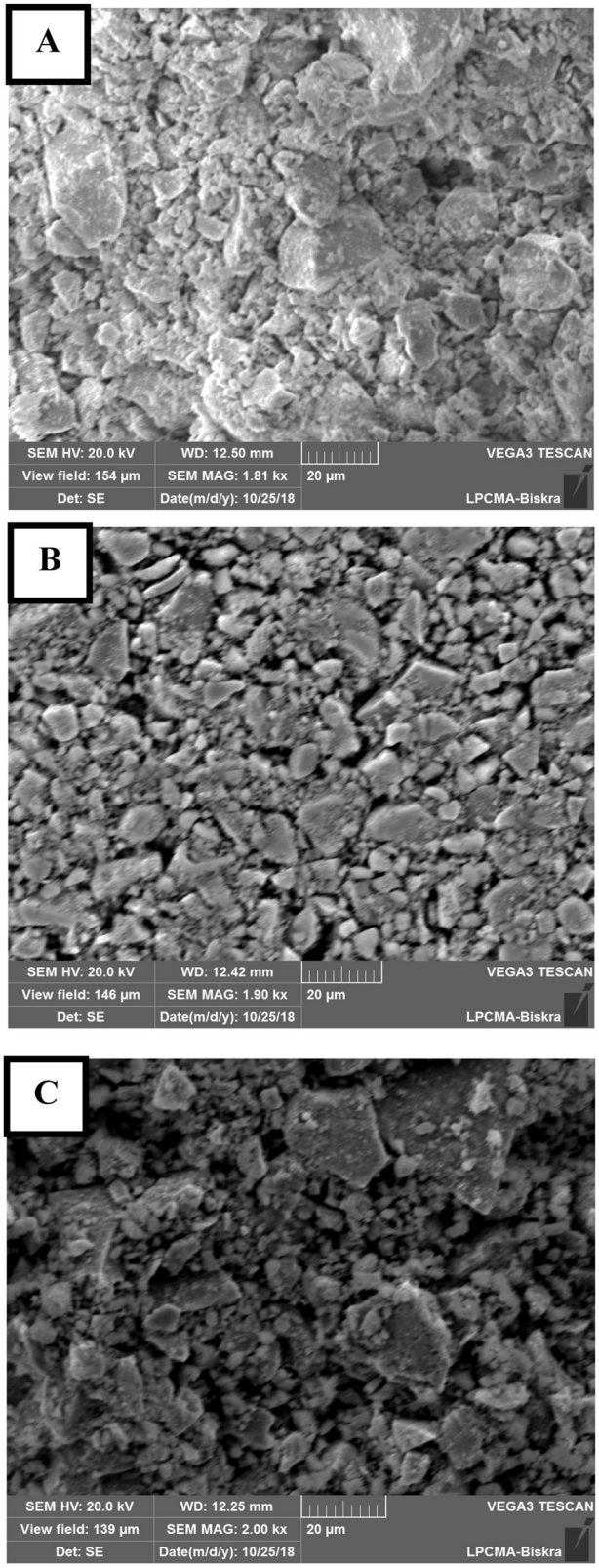

Fig. 2 SEM images of LF: **a** LFZ10; **b** LFZ20; **c** powders calcined at 750 °C

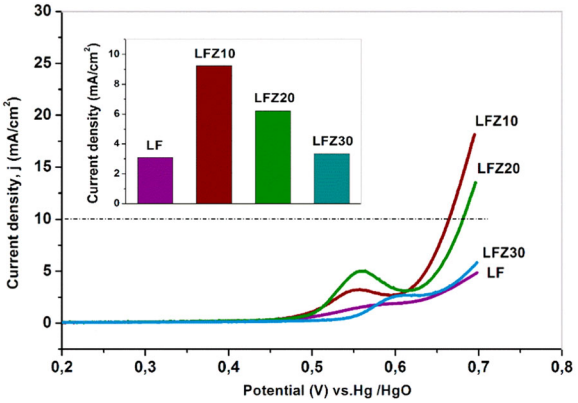

Fig. 3 Linear sweep voltammetry measurements of $LaFe_{1-x}Zn_xO_3$ powders in 1 M KOH, at a scan rate of 50 mV/s; inset shows the OER current at 0.66 V vs. Hg/HgO

3.3 Electrocatalytic properties of $LaFe_{1-x}Zn_xO_3$ catalysts

3.3.1 Oxygen evolution activity

The linear sweep voltammograms of $LaFe_{1-x}Zn_xO_3$ ($0.0 \leq x \leq 0.3$) electrodes in the potential region 0.0–0.7 V vs. Hg/HgO in 1 M KOH with a scan rate of 50 mV s^{-1} are presented in Fig. 3. It is observed that these electrodes have a qualitatively similar behavior. Each voltammogram exhibits only one anodic peak (520 mV ≤ Epa ≤ 576 mV) related to the Ni(II)/Ni(III) redox couple [25, 26]. The shift in the position of redox peaks at lower potential region may be ascribed to the synergistic interaction between Ni metal and $LaFe_{1-x}Zn_xO_3$ catalysts [25–27]. Thus, pure Ni used as the support in the present study may produce oxidation-reduction (Ni^{2+}/Ni^{3+}) reaction during the anodic cycling condition owing to the electrolyte contact through pores, cracks, and so on [27, 28]. However, the observed redox peaks on the oxide films on Ni have not been originated from the catalytic films but were produced from the oxidation of the Ni support [28]. In all cases during a forward scan, these peaks appear just prior to the onset of oxygen evolution with the slight shift toward high potentials. Both the OER onset potential and the overpotential (defined as the potential at the current density of 10 mA cm^{-2}) increase according to the following order: LFZ10 < LFZ20 < LFZ30 < LF, which pointed out clearly that the better electroactivity toward the OER can be achieved with LFZ10 electrode. The value of overpotential required to achieve a current density of 10 mA cm^{-2} for LFZ10 is ~677 mV which is comparable to data already reported in the literature for analogous systems, $La_{0.2}Sr_{0.8}FeO_3$ (~0.66 V) [29], $CaFeO_3$ (~0.81 V) [1], and $GdFeO_3$ (~0.68 V) [30].

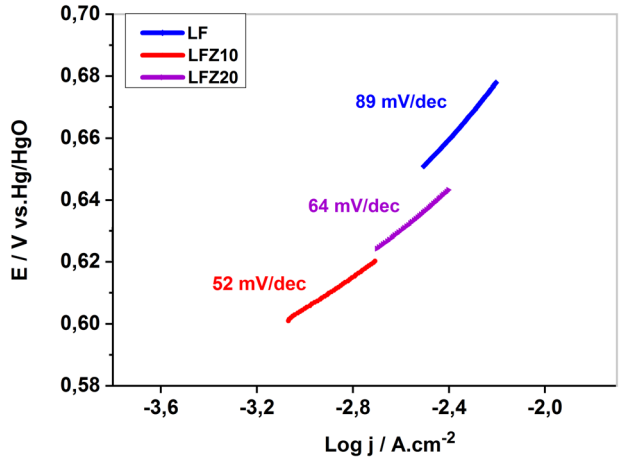

Fig. 4 Tafel plots of $LaFe_{1-x}Zn_xO_3$ powders

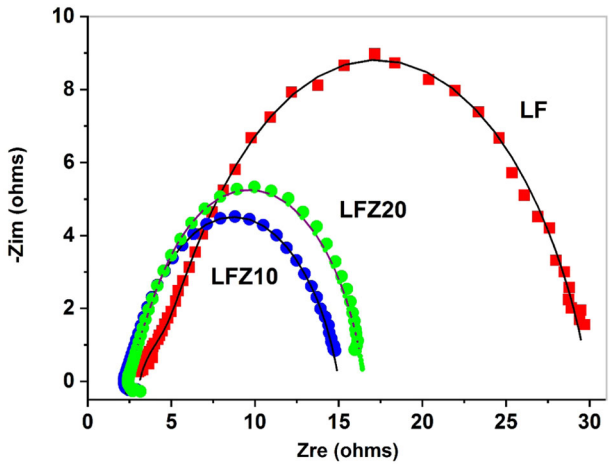

Fig. 5 Complex impedance (Nyquist) of LF, LFZ10, and LFZ20 electrodes in 1 M KOH solution at 25 °C, $E = 0.64$ V. The experiment data are represented by discrete symbols and the simulated impedance reponse is represented by continuous line

On the other hand, the addition of zinc allowed to raise the current density which is approximately three times higher for LFZ10 than LF at $E = 0.66$ V. Indeed at this potential, the LFZ10 catalyst delivers a highest current density ~9.02 mA cm^{-2} compared with all compositions. This is possibly due to the substitution of a transition metal iron by zinc leading to the formation of cation vacancies, which are the result of the high solubility of Zn in KOH solution. This result was also reported by previous works indicating that the addition of zinc generates metal vacancies, defective sites, and hydroxylation, which enhances the OER performance of catalysts [31, 32].

At higher zinc content ($x > 0.1$), it decreases strongly to reach a current density ~3.0 mA cm^{-2} for $x = 0.3$, which is close to that obtained for LF. This indicates probably that the apparition of the secondary phase ZnO which becomes more intense for higher zinc content has an inhibition effect on OER performance [33].

Recently, similar result was also reported in $La_{1-x}Sr_xNiO_3$ [34]. It has been shown that the $SrCO_3$ impurity is inactive for the OER and blocks the active site of electrocatalysts, which negatively impacts the electrocatalytic activity.

Kinetic parameters of the OER, for pure and zinc-doped perovskite electrodes in 1 M KOH at 25 °C, are recorded at a slow scan rate 0.2 mV s^{-1} (Fig. 4). The obtained Tafel plots of LF, LFZ10, and LFZ20 electrocatalysts are 89, 52, and 64 mV dec^{-1}, respectively. This result indicates that the electrode LFZ10 exhibits a better performance in the OER and is consistent with LSV findings.

3.3.2 Electrochemical impedance spectroscopy

EIS was used to study the OER kinetics properties exhibited by the oxide films. A typical complex plane diagram for the active oxide $LaFe_{1-x}Zn_xO_3$ ($0.0 \le x \le 0.2$) at a constant potential $E = 0.64$ V is presented in Fig. 5. The experiment data are represented by discrete symbols and the simulated impedance reponse is represented by continuous line. The two circuit description codes, $R_s(Q_fR_f)(Q_{dl}R_{ct})$ and $LR_s(Q_fR_f(C_{dl}R_{ct}))$ for LF, LFZ10, and LFZ20, respectively, are used to simulate the EIS data and estimate the corresponding circuit parameters. A good agreement is obtained between simulated and experimental curves.

The best fit values of the circuit parameters are shown in Table 1. It can be observed that the resistance of charge transfert increases with the substitution degree from $x = 0.1$ to 0.2, which is in agreement with the findings from LSV indicating that the higher electroactivity is achieved for LFZ10.

3.3.3 Stability test

Long-term stability is an important feature for catalysts that can be used in practical applications. In this aim, LF and LFZ10 electrodes stability was studied under OER conditions. Figure 6 presents the overpotential of LF and LFZ10 required to achieve 3 and 10 mA cm^{-2}, respectively, during 1000 continuous cycles. The choice of using two different current densities is justified by the fact that it is not possible to estimate the overpotential at the common current density for the two samples in the first cycle. In the case of LF sample, the overpotential decreases continuously during the 1000 cycle stability test, which is probably due to the porous nature of this electrode [35]. Two distinct regions are observed corresponding to 100–400, 400–1000 cycles, with a decrease of the overpotential by 60 and 110 mV, respectively. This indicates that after 1000 cycles, this electrode was activated, remains stable, and even more it performs better in the OER domain. For the second sample LFZ10, after the first 100 consecutive cycles, an increase of

Table 1 Values of the equivalent circuit parameters for oxide electrodes in 1 M KOH at 0.64 V

Electrode	R_s (Ω)	$Q_1 \times 10^{-3}$ ($\Omega^{-1}S^n$)	n_1	R_1 (Ω)	$Q_2 \times 10^{-3}$ ($\Omega^{-1}S^{n2}$)	n_2	R_2 (Ω)
LF	3.11 ± 0.02	2.85 ± 0.10	0.77 ± 0.04	25.22 ± 0.04	1.78 ± 1.32	0.71 ± 0.21	1.62 ± 0.42
	$L \times 10^{-7}$ (H)	R_s (Ω)	R_f (Ω)	$Q_f \times 10^{-3}$ ($\Omega^{-1}S^n$)	n	R_{tc} (Ω)	$C_{dl} \times 10^{-4}$ (F)
LFZ10	5.42 ± 0.21	2.29 ± 0.01	20.12 ± 0.90	2.81 ± 0.15	0.77 ± 0.02	12.71 ± 0.02	1.10 ± 0.74
LFZ20	5.303 ± 0.22	2.522 ± 0.01	12.56 ± 0.53	2.418 ± 0.14	0.80 ± 0.02	14.00 ± 0.01	1.903 ± 0.42

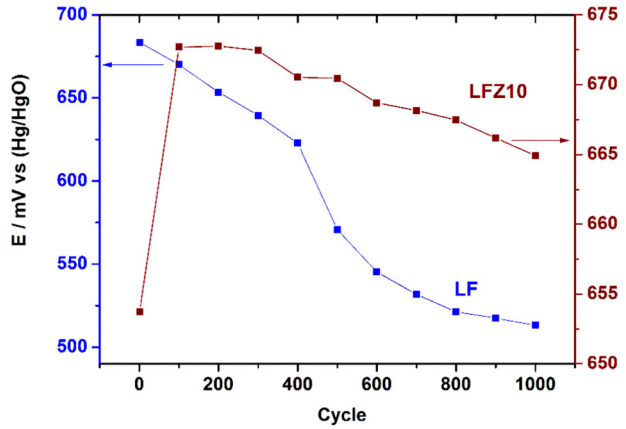

Fig. 6 Change of cell voltage at various points during the 1000 cycle stability tests for LF at 3 mA cm^{-2} and LFZ10 at 10 mA cm^{-2}

overpotential of 19 mV is required to achieve a current density of 10 mA/cm^2, indicating that in this interval the electrode has been desactivated. This is probably due to the surface coverage of oxygen bubbles, formation of film cracks, and so on [36].

This overpotential decreases slightly after the cycle 200, from 19 to 11 mV corresponding to the 1000th cycle, indicating that this electrode has been activated. For comparison an overpotential by 3.41 mV is required for $La_{0.2}Sr_{0.8}FeO_3$ electrode [29], to achieve 3 mA cm^{-2} after 20 cycles, which shows clearly that the very small change in overpotential between 11 and 19 mV, required for LFZ10 to achieve a current density of 10 mA/cm^2 over a large number of cycles indicates a relatively excellent stability of LFZ10 electrode.

4 Conclusion

In summary, Zn-doped $LaFeO_3$ were successfully synthesized by the sol–gel method, employing nitrate salts of lanthanum, iron, zinc as cations precursors, citric acid as a chelating agent. According to X-ray powder diffraction, $LaFe_{1-x}Zn_xO_3$ oxides exhibit a single phase at 750 °C in the range ($0.0 \le x < 0.2$). Two detectable secondary phases $ZnFe_2O_4$ and ZnO were observed for $x = 0.2$ indicating that a solubility is reached for $x < 0.2$. The morphology of samples examined by SEM show a nonuniform grain size distribution and very well pronounced agglomeration of powders. The electrochemical investigation revealed that the substitution of Fe by Zn in the base oxide increased the electrocatalytic activity toward OER. The value being highest with 0.1 mol Zn substitution at $E = 0.66$ V. Moreover, it exhibits a relatively excellent stability after 1000 continuous cycles. Therefore, the LFZ10 oxide can be proposed as an electrode material with a good performance for OER of alkaline water electrolysis process.

Acknowledgements This work was supported by the directorate general of scientific research and technological development DGRSDT of Algeria.

Compliance with ethical standards

Conflict of interest The authors declare that they have no conflict of interest.

Publisher's note Springer Nature remains neutral with regard to jurisdictional claims in published maps and institutional affiliations.

References

1. Sankannavar R, Sarkar A (2018) The electrocatalysis of oxygen evolution reaction on $La_{1-x}CaxFeO_{3-\delta}$ perovskites in alkaline solution. Int J Hydrog Energy 43:4682–4690. https://doi.org/10.1016/j.ijhydene.2017.08.092
2. Carmo M, Fritz DL, Mergel J, Stolten DA (2013) comprehensive review on PEM water electrolysis. Int J Hydrog Energy 38:4901–4934. https://doi.org/10.1016/j.ijhydene.2013.01.151
3. Dincer I (2012) Green methods for hydrogen production. Int J Hydrog Energy 37:1954–1971. https://doi.org/10.1016/j.ijhydene.2011.03.173
4. Sadooghi P, Rauch R (2015) Experimental and modeling study of hydrogen production from catalytic steam reforming of methane mixture with hydrogen sulfide. Int J Hydrog Energy 40:10418–10426. https://doi.org/10.1016/j.ijhydene.2015.06.143
5. Pletcher D, Li X (2011) Prospects for alkaline zero gap water electrolysers for hydrogen production. Int J Hydrog Energy 36:15089–15104. https://doi.org/10.1016/j.ijhydene.2011.08.080
6. Lyons MEG, Brandon MP (2008) The oxygen evolution reaction on passive oxide covered transition metal electrodes in alkaline solution part II-cobalt. Int J Electrochem Sci 3:1425–1462
7. Trotochaud L, Boettcher SW (2014) Precise oxygen evolution catalysts: status and opportunities. Scr Mater 74:25–32. https://doi.org/10.1016/j.scriptamat.2013.07.019
8. Wang CC, Cheng Y, Ianni E, Jiang SP, Lin B (2017) A highly active and stableLa0. 5Sr0. 5Ni0. 4Fe0. 6O3-δ perovskite electrocatalyst for oxygen evolution reaction in alkaline media. Electrochim Acta 246:997–1003. https://doi.org/10.1016/j.electacta.2017.06.161

9. Burke MS, Enman LJ, Batchellor AS, Zou S, Boettcher SW (2015) Oxygen evolution reaction electrocatalysis on transition metal oxides and (oxy) hydroxides: activity trends and design principles. Chem Mater 27:7549–7558. https://doi.org/10.1021/acs.chemmater.5b03148
10. Cheng J, Zhang H, Ma H, Zhong H, Zou Y (2009) Preparation of $Ir_{0.4}Ru_{0.6}Mo_xO_y$ for oxygen evolution by modified Adams fusion method. Int J Hydrog Energy 34:6609–6613. https://doi.org/10.1016/j.ijhydene.2009.06.061
11. Ramsundar RM, Debgupta J, Pillai VK, Joy PA (2015) Co_3O_4 nanorods efficient non-noble metal electrocatalyst for oxygen evolution at neutral pH. Electrocatalysis 6:331–340. https://doi.org/10.1007/s12678-015-0263-0
12. Bockris JO, Otagawa T (1984) The electrocatalysis of oxygen evolution on perovskites. J Electrochem Soc 131:290–302. https://doi.org/10.1149/1.2115565
13. Atta NF, Galal A, Ali SM (2012) The catalytic activity of ruthenates $ARuO_3$ (A=Ca, Sr, or Ba) for the hydrogen evolution reaction in acidic medium. Int J Electrochem Sci 7:725–746.
14. Yagi S, Yamada I, Tsukasaki H, Seno A, Murakami M, Fujii H, Chen H, Umezawa N, Abe H, Nishiyama N, Mori S (2015) Covalency-reinforced oxygen evolution reaction catalyst. Nat Commun 6:8249. https://doi.org/10.1038/ncomms9249
15. Takashima T, Ishikawa K, Irie H (2016) Efficient oxygen evolution on hematite at neutral pH enabled by proton-coupled electron transfer. Chem Commun 52:14015–14018. https://doi.org/10.1039/C6CC08379J
16. Takashima T, Ishikawa K, Irie H (2017) Enhancement of oxygen evolution activity of Ruddlesden-Popper-type strontium ferrite by stabilizing Fe^{4+}. J Mater Sci Chem Eng 5:129–141. https://doi.org/10.4236/msce.2017.54005
17. Suntivich J, May KJ, Gasteiger HA, Goodenough JB, Shao-Horn Y (2011) A perovskite oxide optimized for oxygen evolution catalysis from molecular orbital principles. Science 334:1383–1385. https://doi.org/10.1126/science.1212858
18. Andoulsi-Fezei R, Horchani-Naifer K, Férid M (2016) Influence of zinc incorporation on the structure and conductivity of lanthanum ferrite. Ceram Int 42:1373–1378. https://doi.org/10.1016/j.ceramint.2015.09.077
19. Yang M, Li Y, Yu Y, Liu X, Shi Z, Xing Y (2018) Self-assembly of three-dimensional zinc-doped $NiCo_2O_4$ as efficient electrocatalysts for oxygen evolution reaction. Chem Eur J 24:13002–13008. https://doi.org/10.1002/chem.201802325
20. Huang S, Qin H, Song P, Liu X, Li L, Zhang R, Hu J, Yan H, Jiang M (2007) The formaldehyde sensitivity of $LaFe_{1-x}Zn_xO_3$-based gas sensor. J Mater Sci 42:9973–9977. https://doi.org/10.1007/s10853-007-1991-1
21. Dong S, Xu K, Tian G (2009) Photocatalytic activities of $LaFe_{1-x}Zn_xO_3$ nanocrystals prepared by sol–gel auto-combustion method. J Mater Sci 44:2548–2552. https://doi.org/10.1007/s10853-009-3332-z
22. Bhat I, Husain S, Khan W, Patil SI (2013) Effect of Zn doping on structural, magnetic and dielectric properties of $LaFeO_3$ synthesized through sol–gel auto-combustion process. Mater Res Bull 48:4506–4512. https://doi.org/10.1016/j.materresbull.2013.07.028
23. Singh SP, Samuel S, Tiwari SK, Singh RN (1996) Preparation of thin Co_3O_4 films on Ni and their electrocatalytic surface properties towards oxygen evolution. Int J Hydrog Energy 21:171–178. https://doi.org/10.1016/0360-3199(95)00062-3
24. Tiwari SK, Singh SP, Singh RN (1996) Effects of Ni, Fe, Cu, and Cr substitutions for $La_{0.8}Sr_{0.2}CoO_3$ on electrocatalytic properties for oxygen evolution. J Electrochem Soc 143:1505–1510. https://doi.org/10.1149/1.1836670
25. Singh RN, Madhu, Awasthi R, Tiwari SK (2009) Iron molybdates as electrocatalysts for O_2 evolution reaction in alkaline solutions. Int J Hydrog Energy 34:4693–4700. https://doi.org/10.1016/j.ijhydene.2009.04.006
26. Egelund S, Caspersen M, Nikiforov A, Møller P (2016) Manufacturing of a $LaNiO_3$ composite electrode for oxygen evolution in commercial alkaline water electrolysis. Int J Hydrog Energy 41:10152–10160. https://doi.org/10.1016/j.ijhydene.2016.05.013
27. Singh RN, Madhu, Awasthi R, Sinha ASK (2009) Electrochemical characterization of a new binary oxide of Mo with Co for O_2 evolution in alkaline solution. Electrochim Acta 54:3020–3025. https://doi.org/10.1016/j.electacta.2008.12.012
28. Singh RN, Singh JP, Lal B, Thomas MJK, Bera S (2006) New $NiFe_{2-x}Cr_xO_4$ spinel films for O_2 evolution in alkaline solutions. Electrochim Acta 51:5515–5523. https://doi.org/10.1016/j.electacta.2006.02.028
29. She S, Yu J, Tang W, Zhu Y, Chen Y, Sunarso J, Zhou W, Shao Z (2018) Systematic study of oxygen evolution activity and stability on $La_{1-x}Sr_xFeO_{3-\delta}$ perovskite electrocatalysts in alkaline media. Acs Appl Mater Interfaces 10:11715–11721. https://doi.org/10.1021/acsami.8b00682
30. Omari E, Omari M (2019) Cu-doped GdFeO3 perovskites as electrocatalysts for the oxygen evolution reaction in alkaline media. Int J Hydrog Energy 44(54):28769–28779. https://doi.org/10.1016/j.ijhydene.2019.09.088
31. Driess M, Pfrommer J, Azarpira A, Steigert A, Olech K, Menezes P, Duarte RF, Liao X, Wilks RG, Bär M, Schedel-Niedrig T (2016) Superiorly active and long-term stable nickel-based electrocatalysts for water oxidation in alkaline media based on the ZnO:Ni system. ChemCatChem 9(4):672–676. https://doi.org/10.1002/cctc.201600922
32. Menezes PW, Indra A, Bergmann A, Chernev P, Walter C, Dau H, Strasser P, Driess M (2016) Uncovering the prominent role of metal ions in octahedral versus tetrahedral sites of cobalt–zinc oxide catalysts for efficient oxidation of water. J Mater Chem A 4:10014–10022. https://doi.org/10.1039/C6TA03644A
33. Goux A, Pauporté T, Lincot D (2006) Oxygen reduction reaction on electrodeposited zinc oxide electrodes in KCl solution at 70°C. Electrochim Acta 51:3168–3172. https://doi.org/10.1016/j.electacta.2005.09.005
34. Sankannavar R, Sandeep KC, Kamath S, Suresh AK, Sarkar A (2018) Impact of strontium-substitution on oxygen evolution reaction of lanthanum nickelates in alkaline solution. J Electrochem Soc 165:J3236–J3245. https://doi.org/10.1149/2.0301815jes
35. Morimitsu M, Tamura H, Matsunaga M, Otogawa R (2000) Polarization behaviour and lifetime of IrO_2-Ta_2O_5-SnO_2/Ti anodes in p-phenolsulfonic acid solutions for tin plating. J Appl Electrochem 30(4):511–514.
36. Zhen-Hua Z, Wei S, Waqas QZ, Li-Mei C, Ji Y (2018) Highly active and stable synergistic Ir–IrO2 electro-catalyst for oxygen evolution reaction. Chem Eng Comm 205(7):966–974. https://doi.org/10.1080/00986445.2018.1423970